Inorg. Chem. **2007**, *46*, 9968–9974

Systematic Investigation of Lanthanide Phosphonatoethanesulfonate Framework Structures by High-Throughput Methods, $Ln(O_3P–C_2H_4–SO_3)(H_2O)$ (Ln = La–Dy)

Andreas Sonnauer,[†] Christian Näther,[†] Henning A. Höppe,[‡] Jürgen Senker,[§] and Norbert Stock*,[†]

Institute of Inorganic Chemistry, Christian-Albrechts-University, Otto-Hahn-Platz 6/7, D 24118 Kiel, Germany, Institute of Inorganic and Analytic Chemistry, Albert-Ludwigs-University Freiburg, Albertstrasse 21, D 79104 Freiburg, and Department of Inorganic Chemistry I, University of Bayreuth, Universitätsstrasse 30, D 95447 Bayreuth, Germany

Received May 15, 2007

Following the strategy of using polyfunctional phosphonic acids for the synthesis of new metal phosphonates, the flexible organic linker molecule 2-phosphonoethanesulfonic acid, $H_2O_3P–C_2H_4–SO_3H$ (H_3L), was used in a high-throughput (HT) investigation of lanthanide phosphonatoethanesulfonates. Two HT experiments comprising 96 individual hydrothermal reactions were performed to systematically investigate the influence of pH, rare earth ion, molar ratio of Ln^{3+}:H_3L, and the counterion in the system $LnX_3/H_3L/NaOH/H_2O$ with X = NO_3^-, Cl^-, and CH_3COO^-. Whereas under basic conditions $Ln(OH)_3$ is formed, acidic reaction conditions lead to nine isotypic compounds $Ln(O_3P–C_2H_4–SO_3)(H_2O)$ with Ln = La (**1**), Ce (**2**), Pr (**3**), Nd (**4**), Sm (**5**), Eu (**6**), Gd (**7**), Tb (**8**), and Dy (**9**). The crystal size of the compounds is strongly dependent on the ionic radius of the lanthanides and the pH. No significant influence of the counterions of the rare earth salts is observed. For compounds **1**, **2**, **4**, and **5** the crystal structures could be determined from single-crystal X-ray diffraction. The structures are built up from chains of edge-sharing LnO_8 polyhedra that are connected by the phosphonate and sulfonate groups to layers. These layers are linked by the $–CH_2CH_2–$ group to a three-dimensional framework. The compounds **6** and **8** display luminescence in the visible range (intensity maximum 612 and 544 nm, respectively). Thermogravimetric investigations and temperature-dependent X-ray powder diffraction demonstrate the stability of the crystal structure up to 270 °C. Furthermore IR, Raman, and solid-state MAS NMR spectra of **1** and magnetic property measurements of **7** are also presented.

Introduction

A large number of natural and synthetic inorganic−organic hybrid compounds are now known. These hybrid compounds can be classified depending on interactions and arrangement of the inorganic and organic building units.[1] The class of inorganic−organic hybrids ranges from amorphous nanocomposites over self-assembled mesoporous to crystalline hybrid materials. These compounds, mostly based on carboxylates, sulfonates, and phosphonates, are intensively investigated due to their potential applications as sorbents, ion exchangers, catalysts, or charge storage materials.[2,3] Especially porous hybrid compounds based on metal carboxylates and phosphonates have attracted widespread interest in the past few years.[4−8] We are interested in the use of organic building units containing two or more different functional groups for the synthesis of functionalized porous hybrid compounds or bimetallic hybrid systems. So far our

* To whom correspondence should be addressed. E-mail: stock@ac.uni-kiel.de. Tel: +49-431-880-1675. Fax: +49-431-880-1775.
[†] Christian-Albrechts-University.
[‡] Albert-Ludwigs-University Freiburg.
[§] University of Bayreuth.

(1) Sanchez, C.; Julian, B.; Belleville, P.; Popall, M. *J. Mater. Chem.* **2005**, *15*, 3559.
(2) Clearfield, A. Metal Phosphonate Chemistry. In *Prog. Inorg. Chem.* John Wiley: New York, 1998; Vol. 47, pp 371−510.
(3) Cheetham, A. K.; Férey, G.; Loiseau, T. *Angew. Chem., Int. Ed.* **1999**, *38*, 3268.
(4) Li, H.; Eddaoudi, M.; O'Keeffe, M.; Yaghi, O. M. *Nature* **1999**, *402*, 276.
(5) Latroche, M.; Suble, S.; Serre, C.; Mellot-Draznieks, C.; Llewellyn, P. L.; Lee, J.; Chang, J.; Jhung, S. H.; Férey, G. *Angew. Chem., Int. Ed.* **2006**, *45* (48), 8227.
(6) Bauer, S.; Müller, H.; Bein, T.; Stock, N. *Inorg. Chem.* **2005**, *44*, 9464.
(7) Biemmi, E.; Bein, T.; Stock, N. *Solid State Sci.* **2006**, *8*, 363.
(8) Serre, C.; Groves, J. A.; Lightfoot, P.; Slawin, A. M. Z.; Wright, P. A.; Stock, N.; Bein, T.; Haouas, M.; Taulelle, F.; Férey, G. *Chem. Mater.* **2006**, *18*, 1451.

10.1021/ic7009397 CCC: $37.00
Published on Web 10/12/2007

focus has been on the use of phosphonocarboxylic and iminobis(methylphosphonic) acids ($(H_2O_3P-CH_2)_2N-R$).[6,9] Although a large number of metal phosphonates and metal sulfonates have been reported in the literature,[2,3] mixed phosphonates have only recently been investigated. All these studies are limited to the use of linker molecules based on phosphonoarylsulfonic acids.[10−13] To the best of our knowledge, no structural investigations using flexible linkers, for example, phosphonoalkylsulfonic acids, have been reported in the literature. Therefore, we synthesized 2-phosphonoethansulfonic acid, $H_2PO_3-C_2H_4-SO_3H$ (H_3L) and started a systematic investigation using H_3L and tri- and divalent metal ions. The solvothermal reactions were carried out in our high-throughput (HT) reactors that permit a fast and systematic investigation of complex parameter spaces while consuming only small amounts of starting materials. This methodology makes use of a multiclave system that allows the investigation of 48 different solvothermal reactions at a time.[14,15] Here we report the study of the system $LnX_3/H_3L/NaOH/H_2O$. Two series of isotypic compounds have been obtained so far. Whereas smaller lanthanide(III) ions (Ln = Ho−Lu, CN = 8, ionic radii = 115.5−111.7 pm)[16] and yttrium(III) led to a series of six isotypic compounds,[17] larger lanthanide(III) ions (Ln = La−Dy, CN = 8, ionic radii = 130.0−116.7 pm)[16] led to the nine isotypic title compounds with the composition $Ln(O_3P-C_2H_4-SO_3)(H_2O)$. TG and temperature-dependent X-ray diffraction measurements were performed to get an insight in the thermal stability of the compounds. IR, Raman, and MAS NMR spectroscopy were used to get additional information on the local structure. Since Ln complexes and lanthanide phosphonates[18] often have interesting luminescent properties, they may find application as safety markers,[19] sensors for UV radiation, or antireflection coatings on silicon solar cells;[20] the luminescence properties of the Eu and the Tb compound were investigated.

Experimental Section

Materials and Methods. 2-Phosphonoethanesulfonic acid was synthesized as previously reported in a two-step nucleophile substitution reaction with triethylphosphite and sodium sulfite starting from 1,2-dibromoethane.[21−23] All other reagents were of analytical grade (Aldrich and Fluka) and were used without further purification. HT X-ray analysis was carried out in transmission geometry using a STOE HT powder diffractometer equipped with a linear position sensitive detector (PSD) system.[15] MIR spectra were recorded on an ATI Matheson Genesis in the spectral range 4000−400 cm^{-1} using the KBr disk method. FT-Raman spectra were recorded on a Bruker IFS 66 FRA 106 in the range of 0−3300 cm^{-1} using a Nd/YAG laser (1064 nm). Thermogravimetric (TG) analyses were carried out in nitrogen (75 mL/min, 30−700 °C, 4 °C/min) using a NETSCH STA 409 CD analyzer. ^1H and ^{31}P MAS NMR spectra were recorded with at a DSX Avance 400 FT NMR spectrometer (Bruker). The sample was contained in a 4 mm ZrO_2 rotor mounted in a standard double-resonance 4 mm MAS probe (Bruker). The ^1H and ^{31}P chemical shifts are referenced with respect to TMS and phosphoric acid (85% aq), respectively. The spinning frequency was adjusted to 12 kHz. Data collection was performed applying a single-pulse excitation and broadband proton decoupling using a SPINAL-64 sequence.[24] The SEM micrographs were obtained using a Phillips ESEM XL 30 hot cathode scanning electron microscope equipped with an energy dispersive X-ray (EDX) EDAX analyzer for elemental analysis. Magnetic susceptibility measurement for compound **7** was performed using a magnetic balance B-SU 20 (Bruker) at 15 kG in the temperature range of 80−316 K. Photoluminescence analyses for powders of compound **6** and **8** were performed at room temperature on a Perkin-Elmer LS55 fluorescence spectrometer equipped with a Xe discharge lamp (equivalent to 20 kW for 8 μs duration) and a gated photomultiplier with modified S5 response. The spectra have been corrected for excitation and emission.

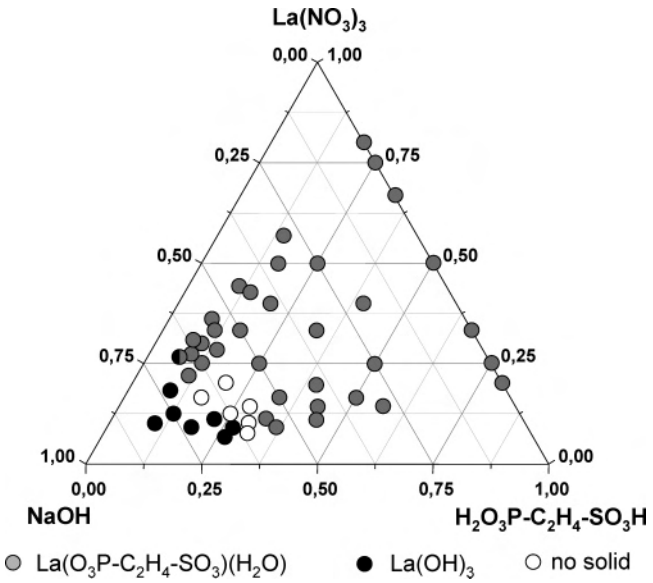

Figure 1. Crystallization diagram of the system $La(NO_3)_3/H_2O_3P-C_2H_4-SO_3H/NaOH/H_2O$. Results are based on powder XRD investigation.

HT Experiments. The system $LnX_3/H_3L/NaOH/H_2O$ was investigated using HT methods. The two HT reactions were performed under hydrothermal conditions at 160 °C for 48 h in a custom-made HT reactor system containing 48 PTFE inserts each with a maximum volume of 300 μL.[14,15] In the first setup, seven molar

(9) Bauer, S.; Bein, T.; Stock, N. *J. Solid State Chem.* **2006**, *179* (1), 145.
(10) Benedetto, A. F.; Squattrito, P. J.; Adani, F.; Montoneri, E. *Inorg. Chim. Acta* **1997**, *260*, 207.
(11) Du, Z. Y.; Xu, H. B.; Mao, J. G. *Inorg. Chem.* **2006**, *45*, 9780.
(12) Du, Z. Y.; Xu, H. B.; Mao, J. G. *Inorg. Chem.* **2006**, *45*, 6424.
(13) Adani, F.; Casciola, M.; Jones, D. J.; Massinelli, L.; Montoneri, E.; Roziére, J.; Vivani, R. *J. Mater. Chem.* **1998**, *8* (4), 961.
(14) Stock, N.; Bein, T. *Solid State Sci.* **2003**, *5*, 1207.
(15) Stock, N.; Bein, T. *Angew. Chem.* **2004**, *116*, 767; *Angew. Chem., Int. Ed.* **2004**, *43*, 749.
(16) Shannon, R. D.; Prewitt, C. T. *Acta Crystallogr.* **1969**, *B25*, 925; Shannon, R. D. *Acta Crystallogr.* **1976**, *A32*, 751.
(17) Isotypic series $M(O_3P-C_2H_4-SO_3)$ with M = Ho−Lu and Y; cell parameters for $Er(O_3P-C_2H_4-SO_3)$: $a = 775.07(13)$ pm, $b = 863.30(17)$ pm, $c = 547.52(10)$ pm, $\beta = 97.235(10)°$, $V = 363.44(17) \times 10^6$ pm^3. The crystal structure determination and the detailed characterization of the compounds is under investigation.
(18) Mao, J. G. *Coord. Chem. Rev.* In press, DOI:10.1016/j.ccr.2007.02.008.
(19) Suyver, F.; Meijerink, A. *Chemisch2Weekblad* **2002**, *98*, 12.
(20) Sá, G. F.; Malta, O. L.; de Mello Donegá, C.; Simas, A. M.; Longo, R. L.; Santa-Cruz, P. A.; da Silva, E. F., Jr. *Coord. Chem. Rev.* **2000**, *196*, 165.
(21) Ford-Moore, A. H.; Williams, H. J. *J. Chem. Soc.* **1947**, 1465.
(22) Montoneri, E.; Ricca, G. *Phosphorus, Sulfur and Silicon* **1991**, *55*, 111.
(23) Sonnauer, A.; Senker, J.; Stock, N. In preparation.
(24) Fung, B. M.; Khitrin, A. K.; Ermolaev, K. *J. Magn. Reson.* **2000**, *142*, 97.

Table 1. Summary of Crystal Data, Intensity Measurement, and Structure Refinement Parameters for La($O_3P-C_2H_4-SO_3$)(H_2O) (**1**), Ce($O_3P-C_2H_4-SO_3$)(H_2O) (**2**), Nd($O_3P-C_2H_4-SO_3$)(H_2O) (**4**), and Sm($O_3P-C_2H_4-SO_3$)(H_2O) (**5**)

	1	**2**	**4**	**5**
space group	$P2_1/c$	$P2_1/c$	$P2_1/c$	$P2_1/c$
a (pm)	839.69(17)	837.68(17)	834.63(17)	832.19(17)
b (pm)	1343.2(3)	1335.2(3)	1320.8(3)	1309.9(3)
c (pm)	725.27(15)	721.21(14)	715.74(14)	711.15(14)
β (deg)	103.51(3)	103.53(3)	103.42(3)	103.42(3)
V (10^6 pm^3)	795.4(3)	784.3(3)	767.5(3)	754.0(3)
formula mass (g/mol)	344.01	345.22	349.34	355.45
total data collect.	5724	5121	2709	6145
unique/obs. data[a)] ($I > 2\sigma(I)$)	1401/1204	1379/1080	1211/829	1822/1501
R(int)	0.1018	0.0559	0.0719	0.0460
R1, wR2 ($I > 2\sigma(I)$)	0.0326, 0.0916	0.0303, 0.0755	0.0363, 0.0754	0.0343/0.0891
R1, wR2 (all data)	0.0374, 0.0942	0.0410, 0.0801	0.0602, 0.0823	0.0421/0.0938
GOF	1.060	0.960	0.932	1.003
Δe min/max [eÅ^{-3}]	−1.645/1.466	−1.546/0.987	−1.336/1.159	−1.943/3.045

[a] Compounds **1**, **2**, and **4** are non-merohedral twinned. The reflections of both individuals were indexed separately using RECIPE, and integration of the intensities was performed using TWIN.[25] By this procedure, overlapping reflections are omitted.

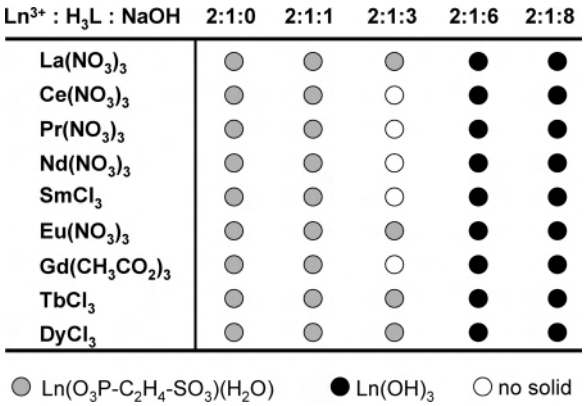

Figure 2. Crystallization diagram of the system $Ln^{3+}/H_2O_3P-C_2H_4-SO_3H/NaOH/H_2O$. Results are based on powder XRD investigation.

ratios of La^{3+}:H_3L (1:1, 1:2, 1:3, 1:4, 2:1, 3:1, and 4:1) were used, and the NaOH content was increased in different steps from 0 to 10 mol equiv based on the amount of H_3L. The results of the HT experiment are given in Figure 1. The best crystallinity of the reaction product was observed in the reactions containing La^{3+} and H_3L in the molar ratio 1:2. Therefore, in the second HT setup, the molar ratio of Ln^{3+}:H_3L was kept constant (1:2) and the NaOH content was increased in five steps (0, 1, 3, 6, and 8 mol equiv based on H_3L). The reactions were performed for the system LnX_3/H_3L/NaOH/H_2O with LnX_3 = $La(NO_3)_3$, $Ce(NO_3)_3$, $Pr(NO_3)_3$, $Nd(NO_3)_3$, $SmCl_3$, $Eu(NO_3)_3$, $Gd(CH_3CO_2)_3$, $TbCl_3$, and $DyCl_3$. The results of the second investigation are shown in Figure 2. Exact amounts of starting materials are given in Tables S1 and S2 in the Supporting Information.

Up-scaling of the Synthesis of Ln($O_3P-C_2H_4-SO_3$)(H_2O). Larger amounts of the compounds were synthesized in culture tubes with temperature-stable caps (DURAN culture tubes 12 × 100 mm D50 GL 14 M.KAP, SCHOTT 261351155). Solutions (2.0 M) of H_3L and LnX_3 (265 μL, 0.53 mmol) were combined and filled up with water to a volume of 2.50 mL. The mixture was heated at 160 °C for 48 h. The precipitate (yield about 40% based on H_3L) was filtered, washed with water, and identified as Ln($O_3P-C_2H_4-SO_3$)(H_2O).

X-ray Structure Analysis. Suitable crystals of the compounds La($O_3P-C_2H_4-SO_3$)(H_2O) (**1**), Ce($O_3P-C_2H_4-SO_3$)(H_2O) (**2**), Nd($O_3P-C_2H_4-SO_3$)(H_2O) (**4**), and Sm($O_3P-C_2H_4-SO_3$)(H_2O) (**5**) were carefully selected from the HT experiments using a polarizing microscope. X-ray diffraction measurements were performed on a STOE IPDS diffractometer equipped with a fine-focus sealed tube (Mo Kα radiation, λ = 71.073 pm). For absorption correction, the programs XRed and X-Shape were used.[25] The crystal structures were solved by direct methods with SHELXS-97 and refined using SHELXL-97.[26] Compounds **1**, **2**, and **4** are non-merohedral twinned. The reflections of both individuals were indexed separately using RECIPE and integration of the intensities was performed using TWIN.[25] By this procedure, overlapping reflections are omitted. Experimental data and results of the structure determination of compounds **1**, **2**, **4**, and **5** are given in Table 1. Selected bond distances are summarized in Table 2. For compound **2** and **5** the hydrogen atoms of the water molecule could be unequivocally localized from the difference Fourier map, the hydrogen bond distances and angles are given in Table S3. The Cambridge Crystallographic Data Center (CCDC) 645749−645752 contains the supplementary crystallographic data for this paper. These data

Table 2. Selected Bond Distances for Compounds **1**, **2**, **4**, and **5**

	1		
P1−O1	150.5(4)	La1−O1	235.2(3)
P1−O2	153.5(3)	La1−O2	251.6(3)
P1−O3	153.5(3)	La1−O3	250.9(3)
S1−O4	145.6(4)	La1−O5	254.7(3)
S1−O5	146.9(4)	La1−O6	258.3(4)
S1−O6	145.7(3)	La1−O7	247.8(4)
	2		
P1−O1	149.1(4)	Ce1−O1	234.4(4)
P1−O2	153.6(4)	Ce1−O2	248.1(4)
P1−O3	154.0(4)	Ce1−O3	249.1(4)
S1−O4	145.5(4)	Ce1−O5	256.5(4)
S1−O5	145.9(4)	Ce1−O6	250.8(4)
S1−O6	147.2(4)	Ce1−O7	244.7(4)
	4		
P1−O1	150.7(7)	Nd1−O1	229.6(7)
P1−O2	153.3(6)	Nd1−O2	246.6(6)
P1−O3	153.6(6)	Nd1−O3	247.1(6)
S1−O4	147.2(7)	Nd1−O5	254.0(7)
S1−O5	145.6(6)	Nd1−O6	247.7(7)
S1−O6	147.6(6)	Nd1−O7	240.1(7)
	5		
P1−O1	150.7(4)	Sm1−O1	227.2(4)
P1−O2	154.0(4)	Sm1−O2	243.3(4)
P1−O3	154.7(4)	Sm1−O3	248.9(4)
S1−O4	146.0(4)	Sm1−O5	251.7(4)
S1−O5	145.5(4)	Sm1−O6	245.0(4)
S1−O6	147.1(4)	Sm1−O7	237.6(4)

(25) *XRED version 1.19, X-Shape version 1.06, RECIPE, TWIN*; Stoe and Cie GmbH: Darmstadt, Germany, 1999.
(26) Sheldrick, G. M. *SHELXTL-PLUS Crystallographic System*; Siemens Analytical X-ray Instruments, Inc.: Madison, WI, 1992.

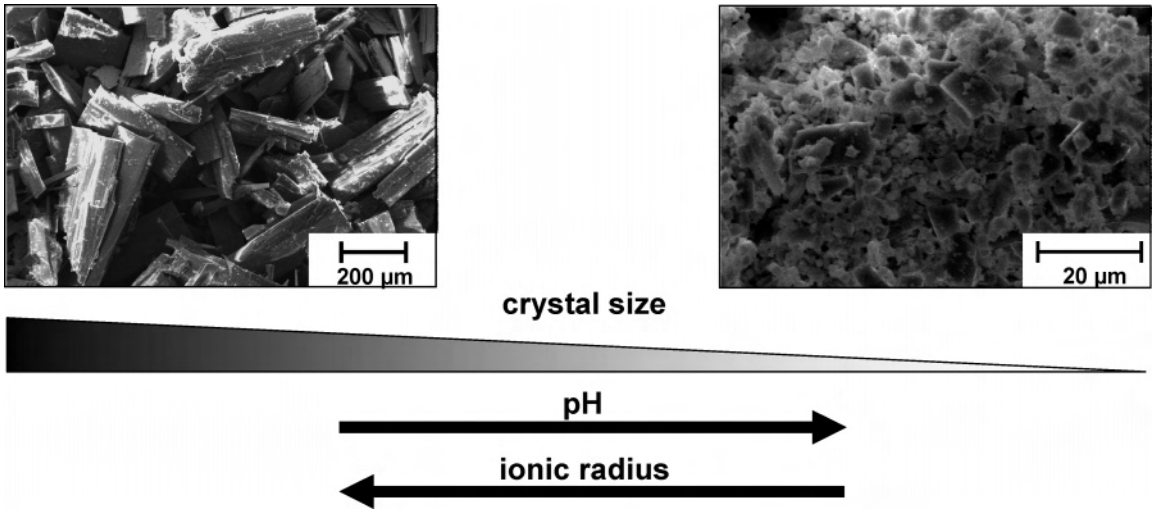

Figure 3. Crystal size dependency of $Ln(O_3P-C_2H_4-SO_3)(H_2O)$ with Ln = La−Dy on pH and ionic radii of the lanthanides.

can be obtained free of charge via the Internet at www.ccdc.cam.ac.uk/conts/retrieving.html (or from the CCDC, 12 Union Road, Cambridge CB2 1EZ, U.K.; fax, +44 1223 336033; e-mail, deposit@ccdc.cam.ac.uk).

Results and Discussion

HT Investigation. The HT methodology allows a fast and systematic investigation of a large part of the parameter space while employing identical reaction conditions such as time, temperature, heating rate, etc. for all 48 reaction vessels. Seven different molar ratios of $M:H_3L$ = 1:1, 1:2, 1:3, 1:4, 2:1, 3:1, and 4:1 were investigated in one experiment in parallel, and the amount of NaOH was increased. In the system $La(NO_3)_3/H_3L/NaOH/H_2O$ only two compounds are observed at the used reaction temperature of 160 °C. Compound **1** is formed over a large region of molar ratios of $M:H_3L$. While the molar ratio M/H_3L of the reaction mixture has almost no influence on the product formation the increase of pH leads to the formation of $La(OH)_3$. The evaluation of the results is shown in Figure 1. In order to learn more about the formation of rare earth phosphonatosulfonates, the system $LnX_3/H_3L/NaOH/H_2O$ for LnX_3 = $La(NO_3)_3$, $Ce(NO_3)_3$, $Pr(NO_3)_3$, $Nd(NO_3)_3$, $SmCl_3$, $Eu(NO_3)_3$, $Gd(CH_3CO_2)_3$, $TbCl_3$, and $DyCl_3$ was investigated by HT methods. For each metal, the molar ratio of $Ln^{3+}:H_3L$ was kept constant at 1:2, and the NaOH content was increased in five steps from 0 to 8 mol equiv based on H_3L. The results are shown in Figure 2. Under acidic conditions all nine rare earth ions lead to the formation of $Ln(O_3P-C_2H_4-SO_3)(H_2O)$. Whereas at molar ratios of $NaOH:H_3L$ (6:2, 8:2) the rare earth hydroxides $Ln(OH)_3$ are obtained. The counterion of the rare earth salts that were employed in this study (i.e., NO_3^-, Cl^-, CH_3OO^-) have no significant influence on the product formation or crystallinity. On the basis of SEM micrographs (Figure 3), a correlation of the crystal size with the pH and the ionic radius of the rare earth ions can be drawn. Thus, large crystals are obtained when the larger rare earth ions are reacted under acidic conditions.

Crystal Structure of $Ln(O_3P-C_2H_4-SO_3)(H_2O)$. Since all title compounds are isotypic, only the crystal structure of **1** will be described as a representative. The asymmetric unit is shown in Figure S1 (Supporting Information). Due to the similar scattering factor of phosphorus and sulfur a differentiation based on the structure refinement is not trivial. This can be unequivocally accomplished by comparing bond lengths with data given in the literature. While in the metal phosphonates $Sm[(O_3PCH_2)_2N(H)C_6H_4COOH]\cdot H_2O$,[27] $GdH[O_3P(CH_2)_3PO_3]$,[28] and $La(O_3PC_6H_5)(HO_3PC_6H_5)$[29] P−O bond lengths in the range 147(2)−155(1) pm are observed, the corresponding S−O bond lengths in the metal sulfonates $La(CH_3SO_3)_3\cdot 2H_2O$[30] and $(C_{10}H_7SO_3)[Pr(C_{10}H_7SO_3)_2(H_2O)_6]\cdot H_2O$[31] are significantly shorter, 143(1)−146(1) pm. These values compare well with the bond lengths observed in our study where P−O and S−O distances of 150.5(4)−153.5(3) and 145.7(3)−146.9(4) pm, respectively, are observed. This assignment is also supported by ^1H and ^{31}P MAS NMR measurements that were performed for the lanthanum compound (Figure S2). In the ^1H spectra two overlapping signals at 6.29 and 2.52 ppm are observed, which can be assigned to the coordinated water molecule and the CH_2 groups, respectively. The ^{31}P spectra show one singulet at 10.73 ppm that indicates the presence of only one crystallographically independent phosphorus atom and no disorder between sulfonate and phosphonate group.

The three-dimensional structure is composed of La^{3+} and 2-phosphonatoethanesulfonate $(O_3P-C_2H_4-SO_3)^{3-}$ ions and one water molecule. The La^{3+} ions are surrounded by eight oxygen atoms. Each rare earth ion is connected to six $O_3P-C_2H_4-SO_3^{3-}$ ions through five P−O−Ln and two S−O−Ln bonds. The full coordination sphere is completed by the H_2O molecule (Figure 4). The oxygen atoms act as end-on (O1, O5, O6) and bridging ligand atoms (O2, O3). Thus, edge-sharing of the LaO_8 polyhedra are observed that lead to the formation of chains along the *c* axis. These chains are

(27) Bauer, S.; Bein, T.; Stock, N. *J. Solid State Chem.* **2005**, *179*, 145.
(28) Serpaggi, F.; Ferey, G. *J. Mater Chem.* **1998**, *8*, 2749.
(29) Wang, R. C.; Zhang, Y.; Hu, H.; Frausto, R. R.; Clearfield, A. *Chem. Mater*. **1992**, *4*, 864.
(30) Wickleder, M. S. *Z. Anorg. Allg. Chem.* **2001**, *627*, 1675.
(31) Ohki, Y.; Suzuki, Y.; Nakamura, M.; Shimoi, M.; Ouchi, A. *Bull. Chem. Soc. Jpn.* **1985**, *58*, 2968.

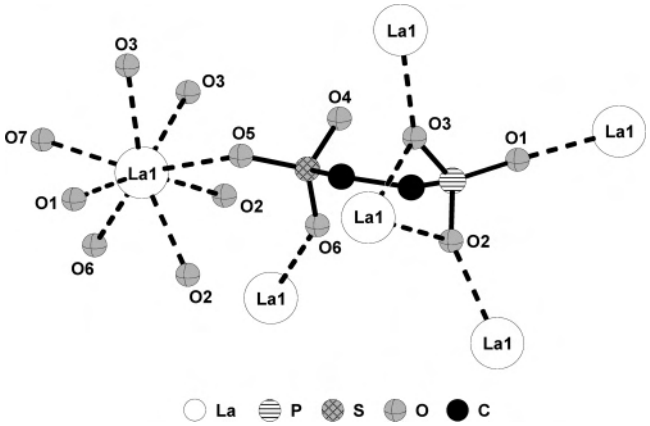

Figure 4. Coordination spheres of lanthanum, phosphonate, and sulfonate groups in compound **1**. Each $O_3P-C_2H_4-SO_3^{3-}$ ion is connected to six La^{3+} ions.

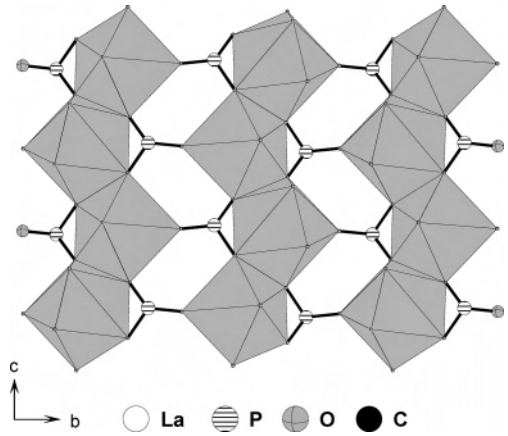

Figure 5. One-dimensional chains of edge-sharing LaO_8 polyhedra along the *c* axis are connected by the sulfonate and phosphonate groups. LaO_8 polyhedra are shaded in gray.

connected to layers by the phosphonate and sulfonate groups (Figure 5). The interconnection of the layers is accomplished through the $-CH_2-CH_2-$ group, and a three-dimensional framework is formed (Figure 6). The structure is further stabilized by hydrogen bonds. Oxygen atom O4 of the sulfonate group acts as a H-acceptor in the hydrogen bond with the coordinated water molecule (O7). The H-atoms could be unequivocally localized in the structure refinement of compounds **2** (Ce) and **5** (Sm) from the difference Fourier map. The hydrogen-bonding scheme is given in Figure S3.

All metal phosphonatosulfonate structures reported in the literature so far are based on phosphonoarylsulfonic acids. Thus, the reaction of *m*-sulfophenylphoshponic acid with various metal salts in the presence of co-ligands (phen, bipy, ect.) led to structures with tetra- or hexanuclear metal phosphonate/sulfonate clusters.[11,12] Furthermore, complex salts based on 4-fluoro-3-sulfophenylphoshponic acid and $[Ni(NH_3)_2(H_2O)_4]^{2+}$ or Na^+ ions have been observed.[10]

Lattice Constants Correlation. As expected, the lanthanide contraction leads to the decrease of the lattice parameters in the isotypic series $Ln(O_3P-C_2H_4-SO_3)(H_2O)$ with Ln = La−Dy. The correlation between the ionic radii and the lattice constants is shown in Figure 7. There is a linear dependency of the lattice constants *a*, *b*, and *c* vs the ionic radius, but the monoclinic angle remains almost

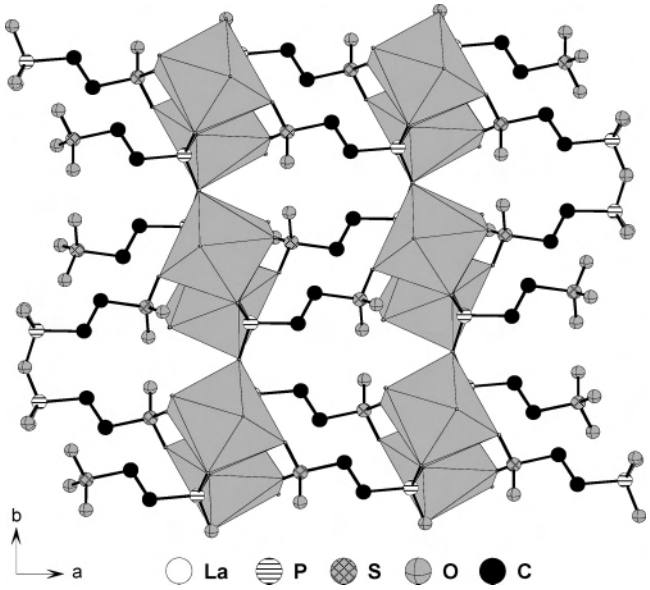

Figure 6. LaO_8 polyhedra sulfonate/phosphonate layers (Figure 4) are interconnected by the $-CH_2CH_2-$ group to a three-dimensional network. LaO_8 polyhedra are shaded in gray.

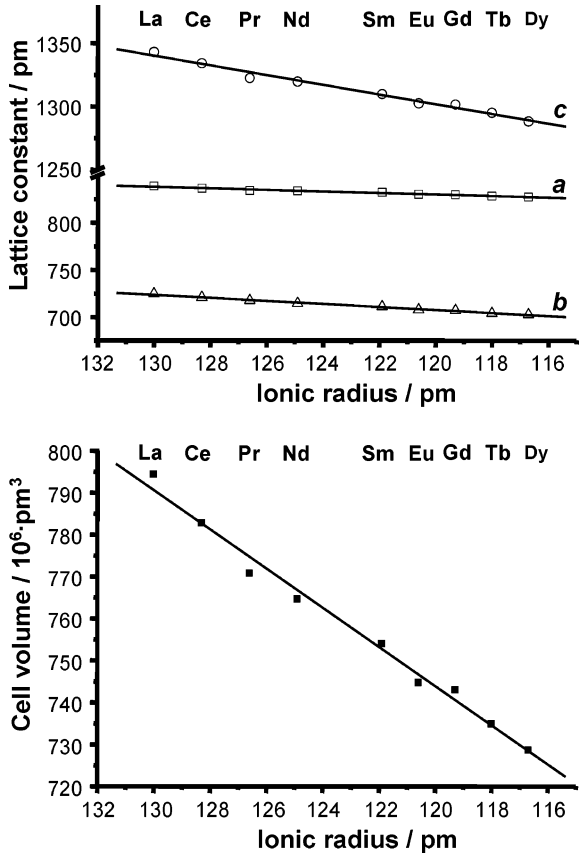

Figure 7. Correlation of the lattice constants *a*, *b*, and *c* and the cell volume *V* in relation to the ionic radius of lanthanoide ions. The decrease of the lattice constant is especially pronounced along the *c* axis.

constant. Along the *c* axis the change is more pronounced, which is due to the edge-sharing LaO_8 polyhedra along this axis. The reduction of the cell parameters is well observed in the powder XRD patterns (Figure S4).

IR and Raman Spectroscopy Study. The title compounds were studied by IR and Raman spectroscopy (Figure S5). All compounds exhibit typical bands in the region between

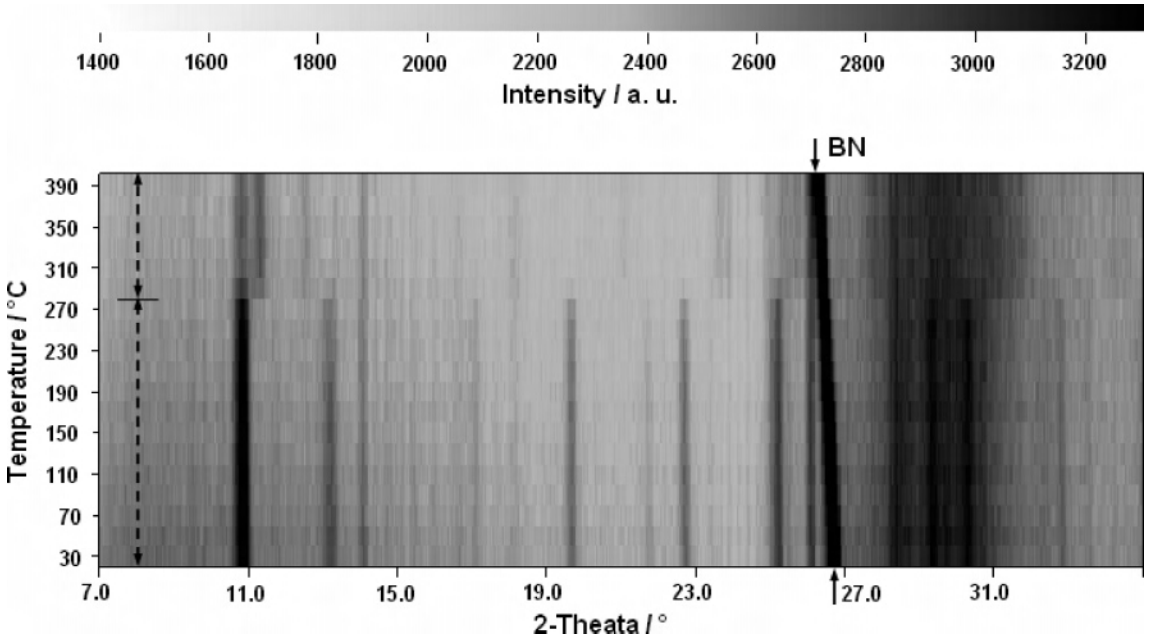

Figure 8. Temperature-dependent X-ray powder diffraction of La($O_3P-C_2H_4-SO_3$)(H_2O) (**1**) in steps of 20 °C. Due to strong X-ray absorption, the sample was diluted with boron nitride BN (reflection is marked with arrows).

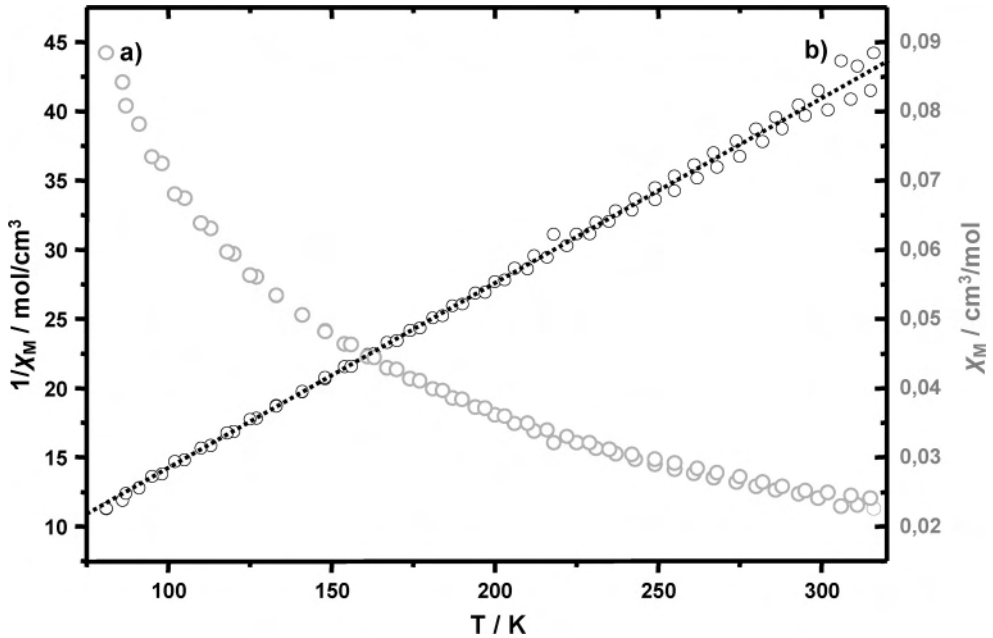

Figure 9. Temperature-dependent plot of a) χ_m and b) $1/\chi_m$ of Gd($O_3P-C_2H_4-SO_3$)(H_2O) (**7**). The dotted line shows the best fit to the Curie−Weiss law.

1250 and 950 cm^{-1} that are due to the P−C, P−O, S−C, and S−O stretching vibrations of the tetrahedral CPO_3 and CSO_3 group. In accordance with the crystallographic results, there is one coordinated water molecule that is involved in hydrogen bonding. Thus, we see a broad band in the IR spectrum at 3267 cm^{-1}. The corresponding deformation band appears at 1664 cm^{-1}. Bands in the region 3001−2919 cm^{-1} are due to CH_2 stretching vibrations. The corresponding CH_2-deformation vibration appears in the IR spectra at 1422 cm^{-1} and in Raman spectra at 1415 cm^{-1}.

Thermal Study. In order to learn more about the thermal stability of the title compound, TG and temperature-dependent X-ray diffraction measurements were performed. The results of TG investigation (Figure S6) show two steps of weight loss for La($O_3P-C_2H_4-SO_3$)(H_2O). The loss of one water molecule per formula unit (observed: −5.30%, calculated: −5.23%) is observed between 270 and 360 °C. The dehydrated sample can be heated up to 400 °C without any weight loss. Above this temperature, the decomposition of the organic molecules takes place. These results correlate well with a temperature-dependent X-ray diffraction investigation (Figure 8). Here the formation of a second crystalline phase is observed around 280 °C, which corresponds to the dehydrated sample.

Magnetic Property Study of Gd($O_3P-C_2H_4-SO_3$)(H_2O). To get an insight into the magnetic properties of **7**, a temperature-dependent magnetic measurement was performed. Figure 9 shows the inverse magnetic susceptibility

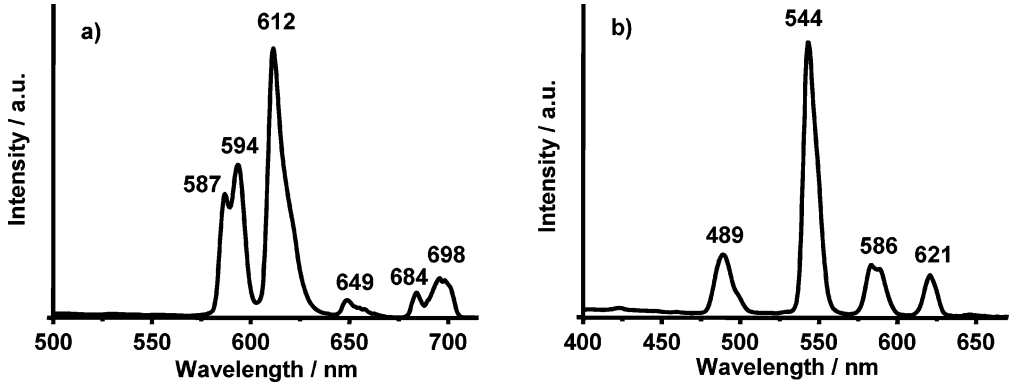

Figure 10. Solid-state emission spectra of (a) **6** (Eu^{3+}) and (b) **8** (Tb^{3+}).

and the susceptibility plotted as a function of temperature. The compound exhibits Curie−Weiss behavior in this temperature range, and the data were least-squares fitted by a Curie−Weiss equation $\chi_M = C/(T - \theta)$ with $C = 7.47$ and $\theta = -5.75$ K. We observed an effective magnetic moment μ_{eff} per metal ion of 7.73 μ_B (6.79 unpaired electrons) which is slightly smaller than the theoretical value of 7.94 μ_B for an f^7 system with seven unpaired electrons.

Luminescent Properties. The solid-state emission spectra from powders of compounds **6** and **8** were measured at room temperature. Compound **6** exhibits several strong characteristic emission bands for isolated europium(III) ions in the visible region excited at 243 nm (Figure 10a). These emission bands are 587 and 594 ($^5D_0 \rightarrow {}^7F_1$), 612 ($^5D_0 \rightarrow {}^7F_2$), 649 ($^5D_0 \rightarrow {}^7F_3$), 684 ($^5D_0 \rightarrow {}^7F_4$), and 696 nm ($^5D_0 \rightarrow {}^7F_4$). Under excitation of 219 nm, compound **8** displays the characteristic emission bands for isolated terbium(III) ions. The spectrum (Figure 10b) shows four emission bands in the visible region at 489 ($^5D_4 \rightarrow {}^7F_6$), 544 ($^5D_4 \rightarrow {}^7F_5$), 586 ($^5D_4 \rightarrow {}^7F_4$), and 621 nm ($^5D_4 \rightarrow {}^7F_3$). The excitation wavelengths were chosen according to the maximum excitation recorded for the strongest emission bands.

Conclusion

Employing our HT methodology, we have investigated the system $LnX_3/H_3L/NaOH/H_2O$ with Ln = La, Ce, Pr, Nd, Sm, Eu, Gd, Tb, and Dy, as well as the use of different counterions ($X = NO_3^-$, Cl^-, CH_3OO^-) under hydrothermal conditions at 160 °C. Acidic reaction conditions lead to Ln-($O_3P-C_2H_4-SO_3$)(H_2O). The used counterions of the rare earth salts have no significant influence on the product formation or crystallinity. In contrast a correlation of the crystal size with the pH and the ionic radius of the rare earth ions can be observed. Thus, large crystals are obtained when the larger rare earth ions are reacted under acidic conditions. The lanthanide contraction leads to a linear decrease of the lattice parameters in the isotypic series. The structural chemistry of metal phosphonosulfonates is strongly determined by the flexibility of the organic group and the presence of additional co-ligands during the synthesis. While the use of phosphonosulfonic acids with rigid organic linker molecules, i.e., phosphonoarylsulfonic acids, together with phen or bipy leads to tetra- or hexanuclear metal−phosphonoarylsulfonate clusters,[11,12] the flexible phosphonoethanesulfonic acid has yielded an extended M−O−M structure with phosphonate and sulfonate groups coordinating to rare earth ions. On the basis of the results of other HT experiments many di- and trivalent cations form crystalline products with the 2-phosphonoethanesuflonic acid. In these compounds, layered and three-dimensional M−O−M structures are observed. These results will be reported soon.

Acknowledgment. The authors thank Inke Jess for thermogravimetric and Maren Rasmussen for magnetic measurement. This work is supported by the DFG-Project STO 643/2-2. H.A.H. thanks the German Chemical Industry Fund FCI (Liebig grant).

Supporting Information Available: Detailed reaction parameters of the HT investigations, powder XRD patterns, TG curve, ^1H and ^{31}P MAS NMR spectra, and IR and Raman spectra. This material is available free of charge via the Internet at http://pubs.acs.org.

IC7009397